Long-term variations of X-ray pulse profiles for the Crab pulsar

Shang, Lunhua

Email:shanglunhua@qxslab.cn

Qian Xuesen Laboratory of Space Technology

2019.06.26

陕西·西安

I. The frequency-dependent behavior of the average pulse profile

II. Long-term variations of radio pulse profile of six pulsars

III. Long-term variations of X-ray pulse profiles for the Crab pulsar

IV. Summary

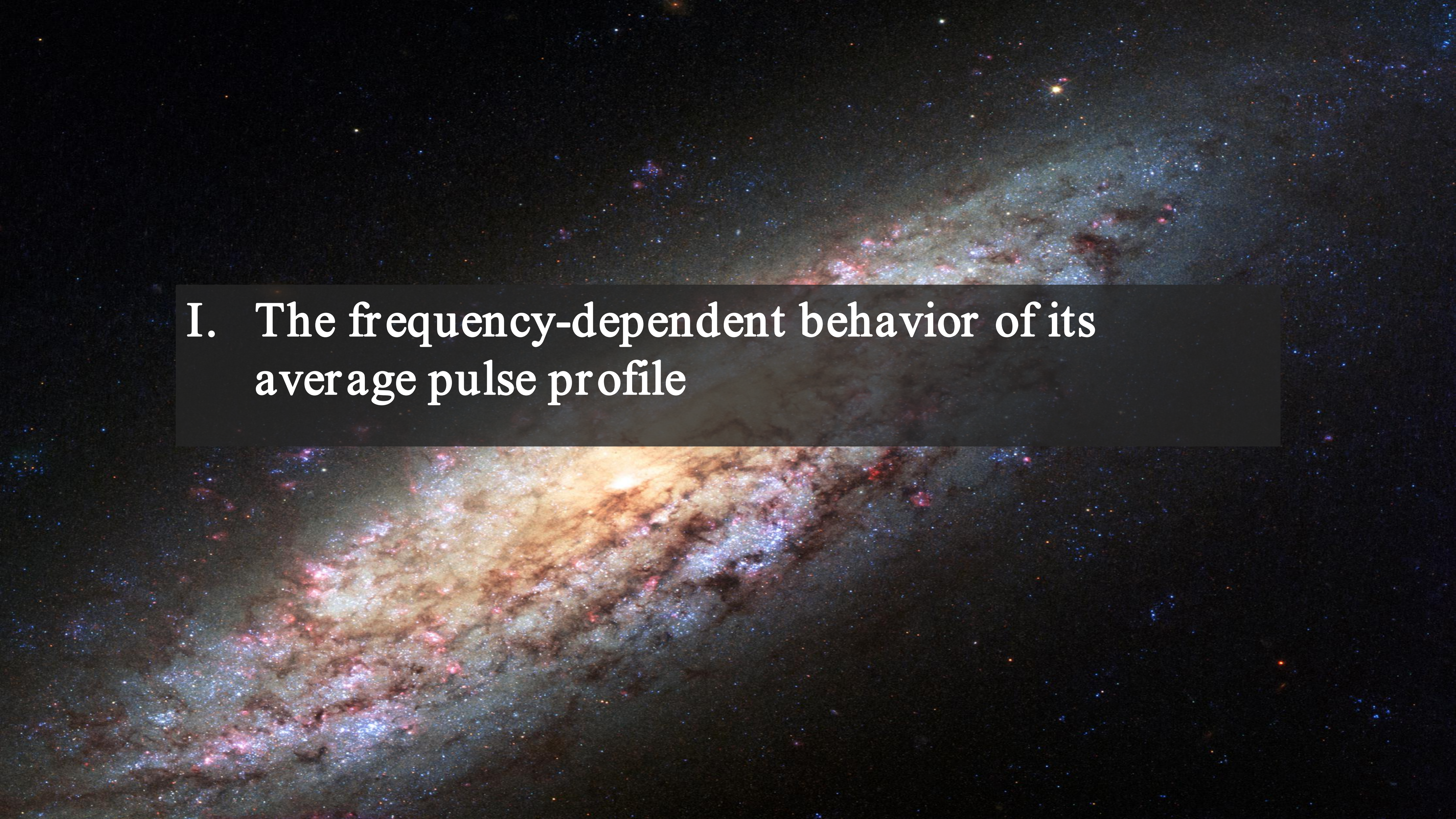

I. The frequency-dependent behavior of its average pulse profile

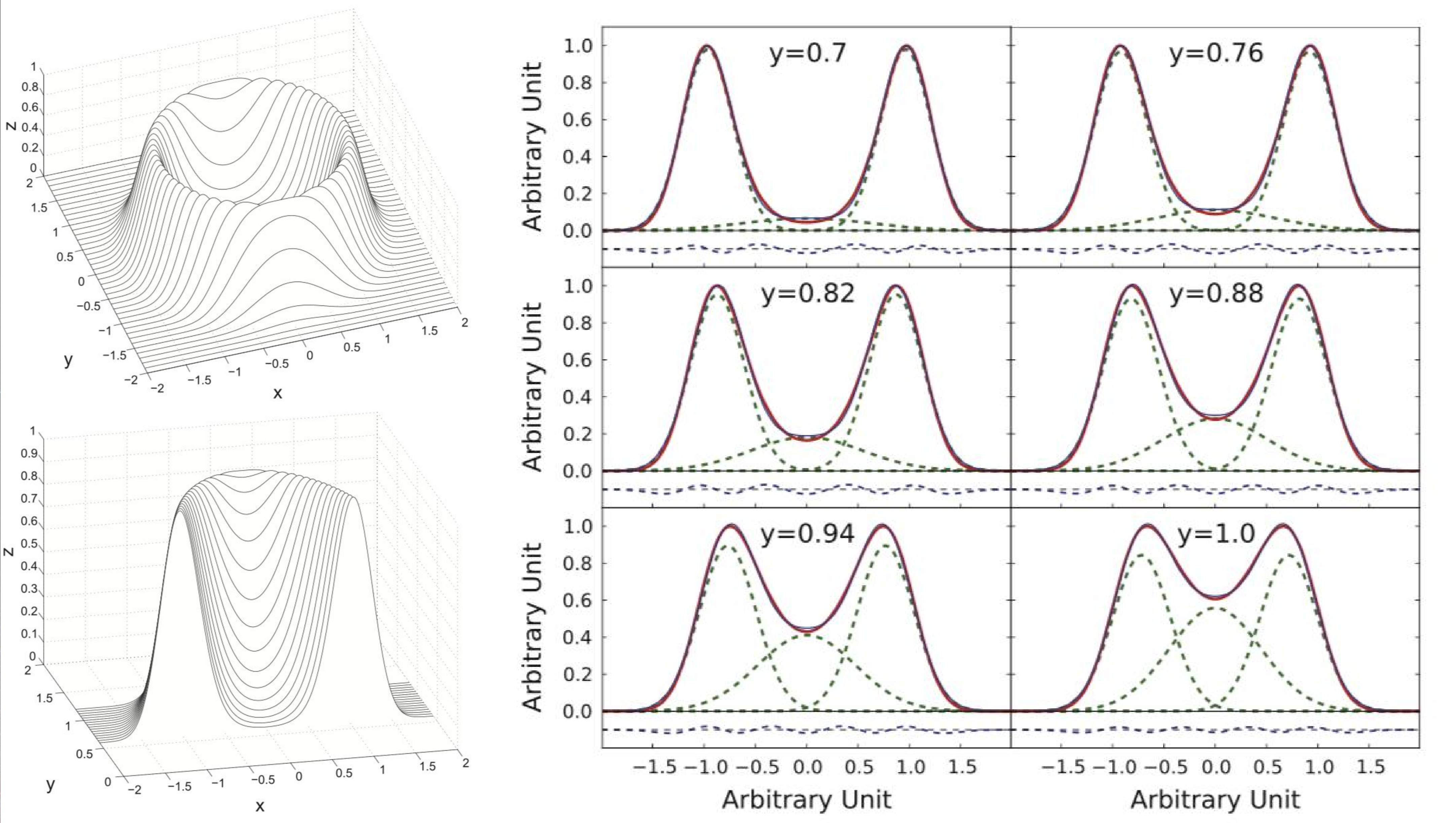

Radiation conal component， cut-out section and component fit (Lu et al. 2016, ApJ.)

M. Kramer 1994, A&A

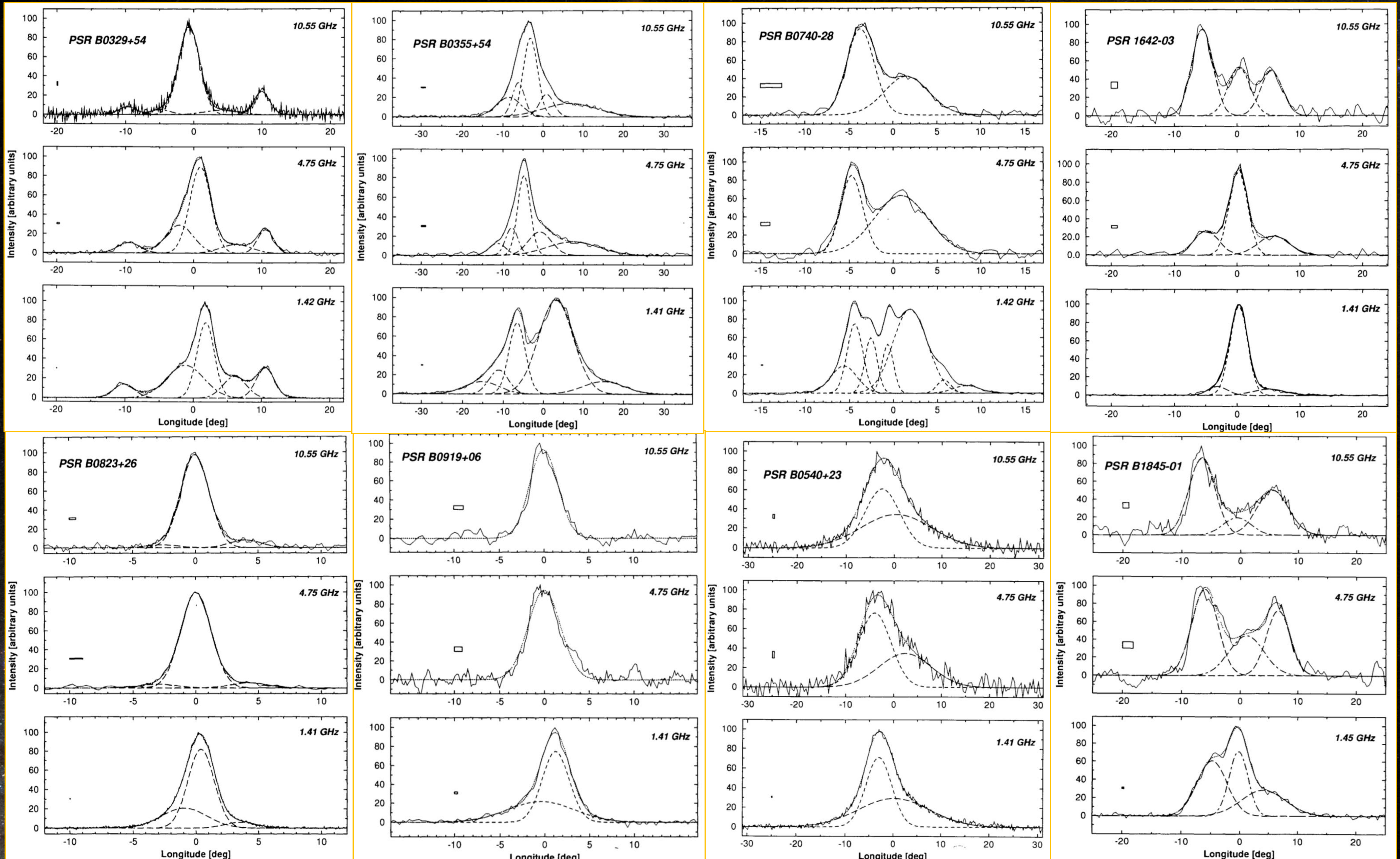

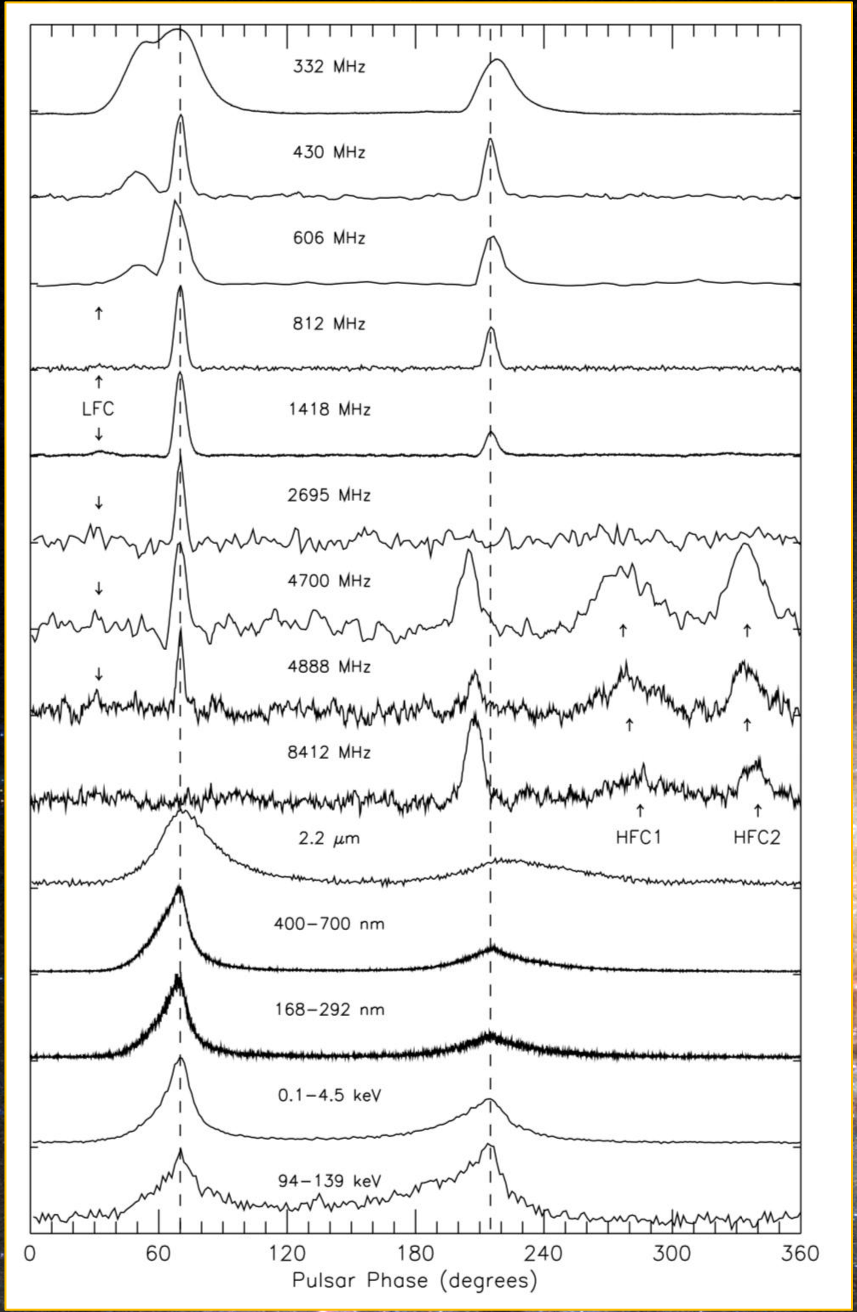

Multifrequency pulse profiles of Crab pulsar (Moffett & Hankins 1996)

- The LFC can be seen from 0.6 to 4.8 GHz, just barely above the noise level at some frequencies.
- At 2.7 GHz, the interpulse disappears, then it reappears at 4.7 GHz, ~10◦ ahead of its low frequency position.
- Then between 8.4 GHz and 2.2 µm, the profile evolves from having only three components, with the main pulse missing, back to two components, with much broader MP and IP.
- The MP and IP dominate emission in the infrared.
- At higher energies, the shape of the MP and IP remains virtually constant.

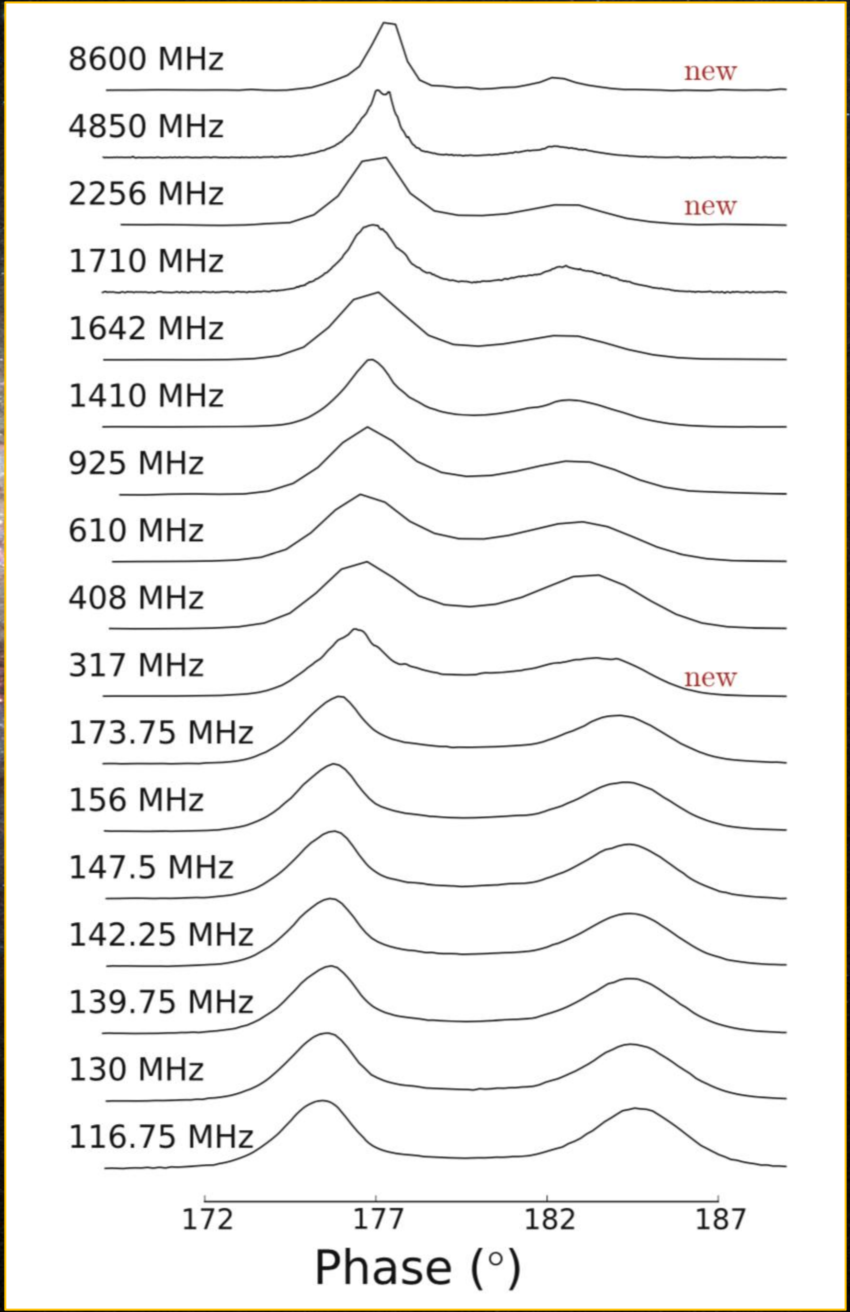

Multi-frequency profile of PSR B1133+16 (Lu et al. 2016)

II. Long-term variations of radio pulse profile of six pulsars

The observed changes in spin-down are indeed directly related to changes in pulse shape.

The integrated profiles at 1400 MHz of six pulsars that show long-term pulse shape changes. For each pulsar, the two traces represent examples of the most extreme pulse shapes observed. The profile drawn in the thick line corresponds to the largest rate of spin-down rate.

Lyne et al. 2010, Science

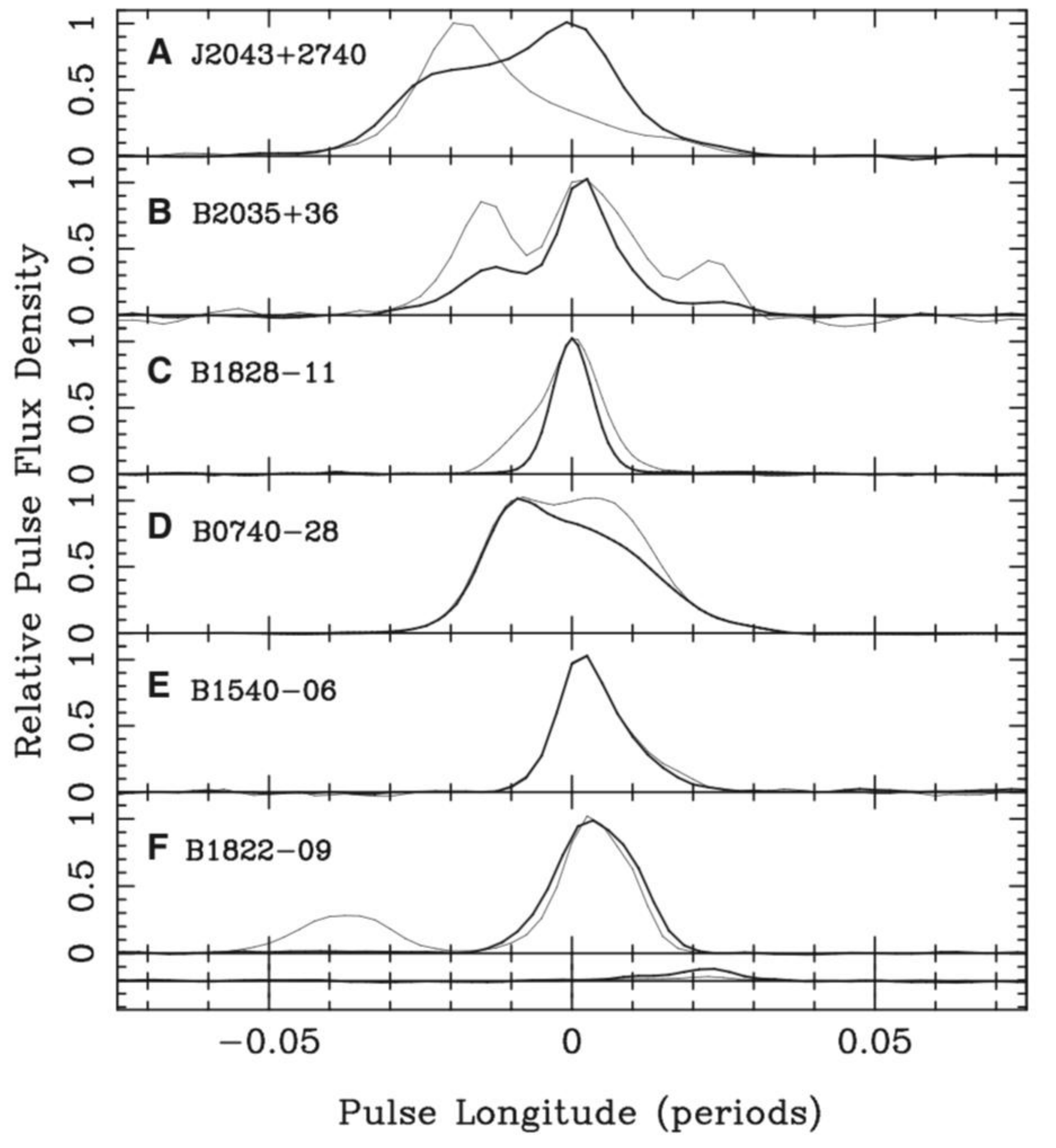

The average value of pulse-shape parameter and spin-down rate measured for six pulsars. The lower trace in each panel (right-hand scale) shows the same values of spin-down rate, whereas the upper trace gives a measure of the pulse shape, with the scale given to the left. W10, W50, and W75 are the full widths of the pulse profile at 10, 50, and 75% of the peak pulse amplitude, respectively

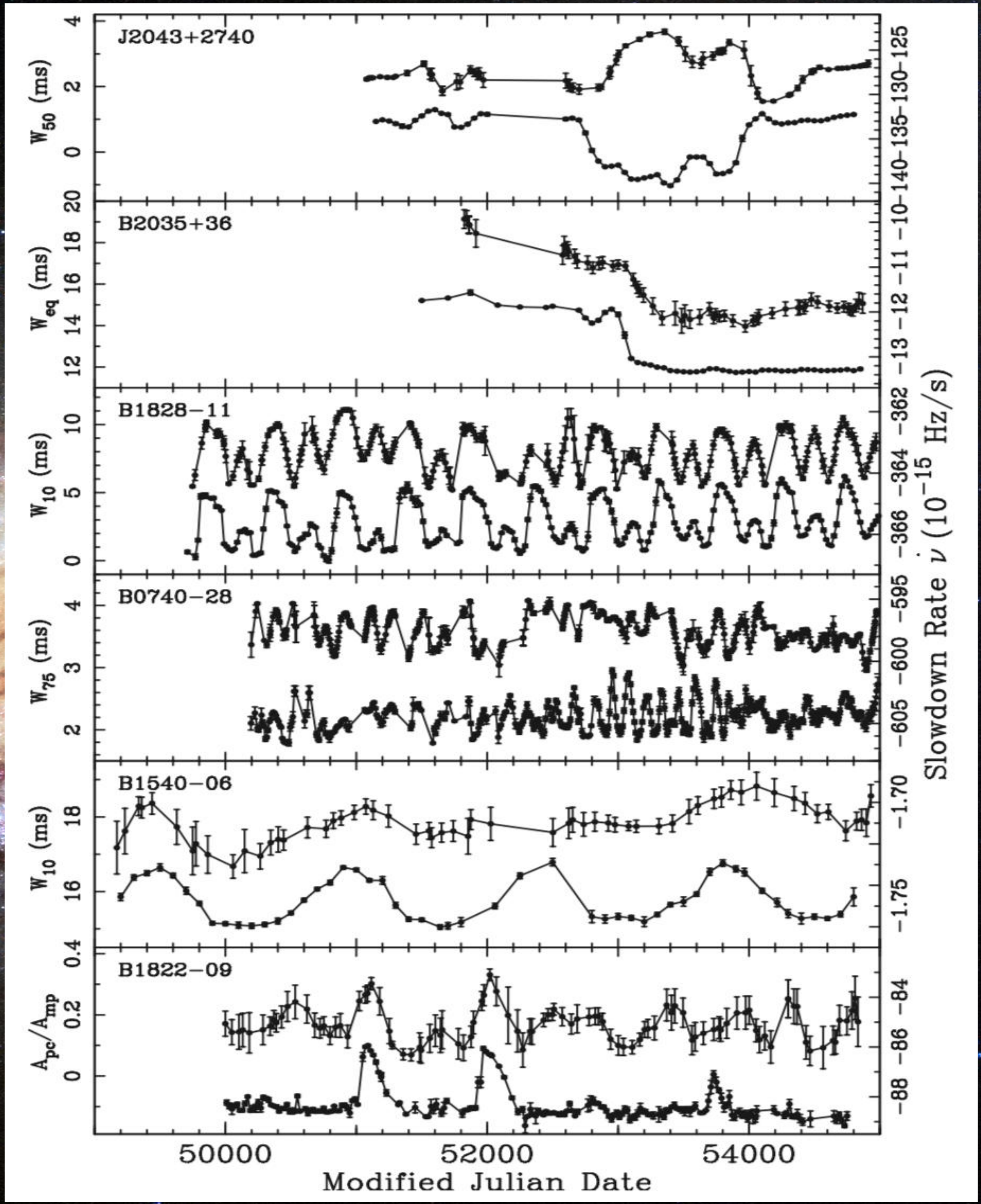

Lyne et al. 2010, Science

III. Long-term variations of X-ray pulse profiles for the Crab pulsar

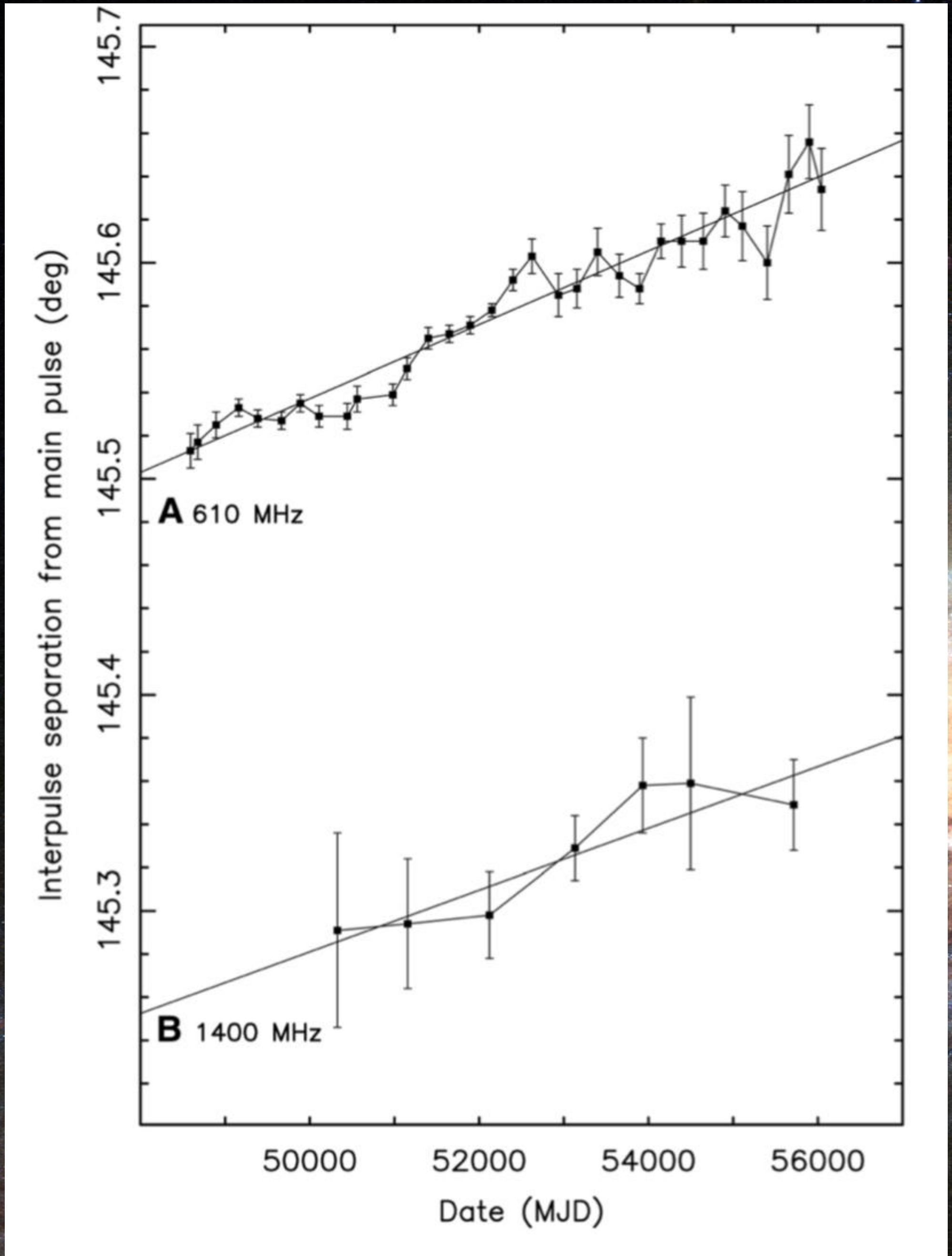

The rotational separation of the IP from the MP，Lyne et al. 2013

- The radio pulse profile has shown a steady increase in the separation of the main pulse and interpulse components at ~ 0.62° per century.
- There are also secular changes in the relative strengths of several components of the profile.
- The changing component separation indicates that the axis of the dipolar magnetic field is moving toward the stellar equator.

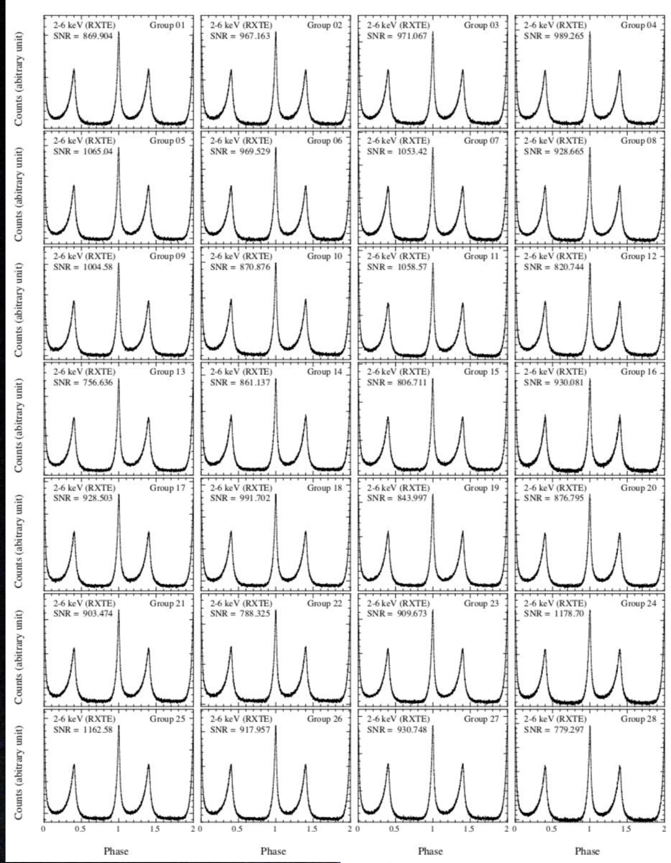

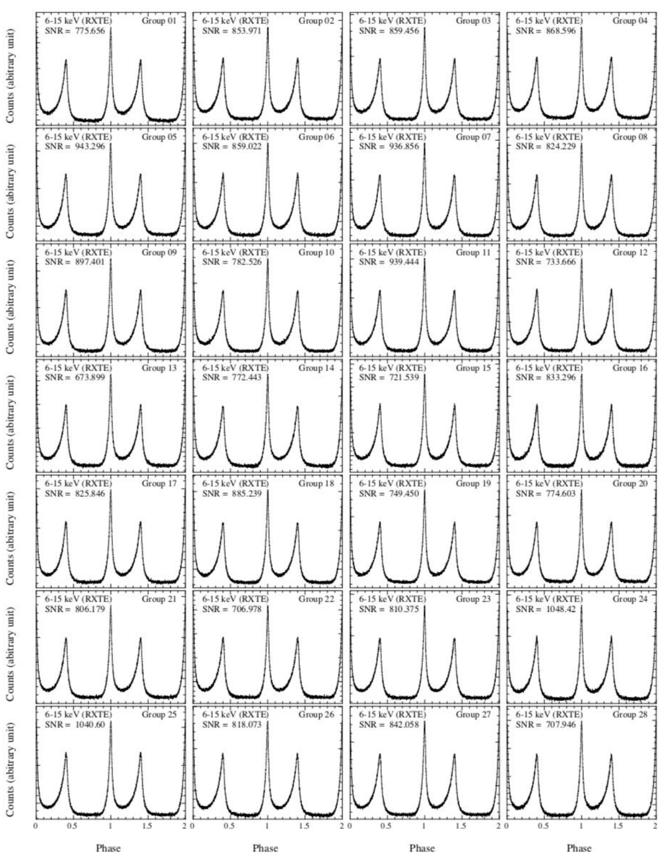

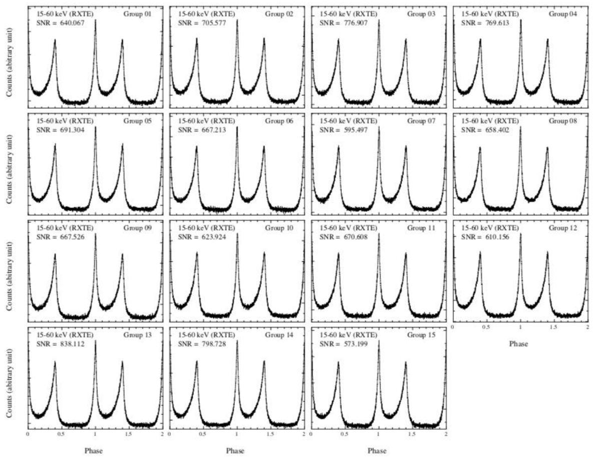

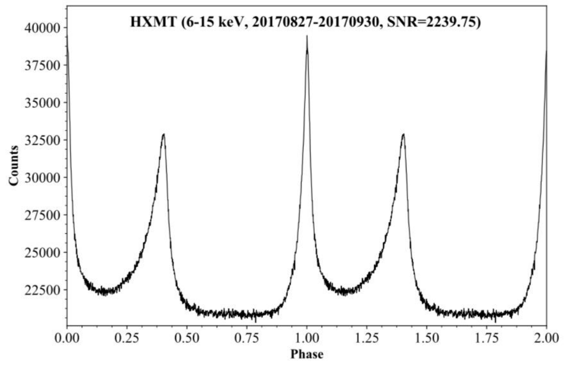

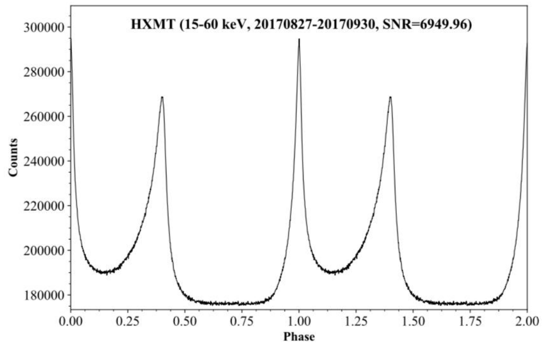

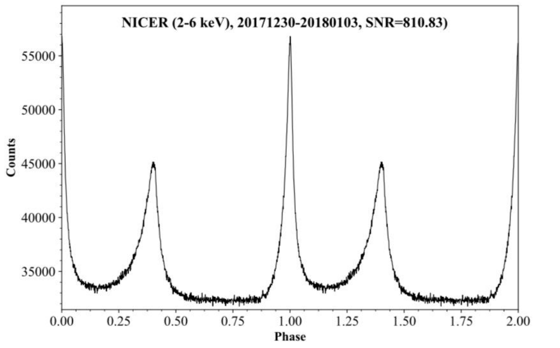

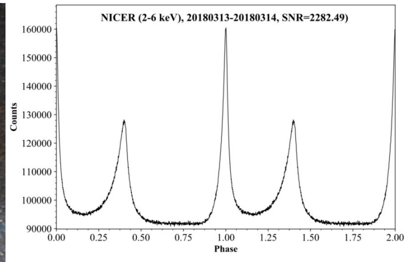

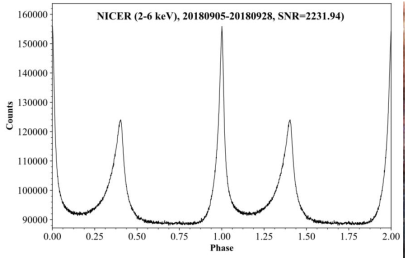

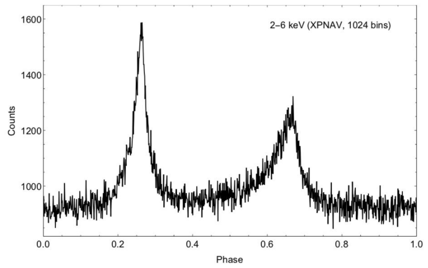

High SNR template pulse profiles with two cycles of the Crab pulsar derived from the RXTE, HXMT, NICER and XPNAV data.

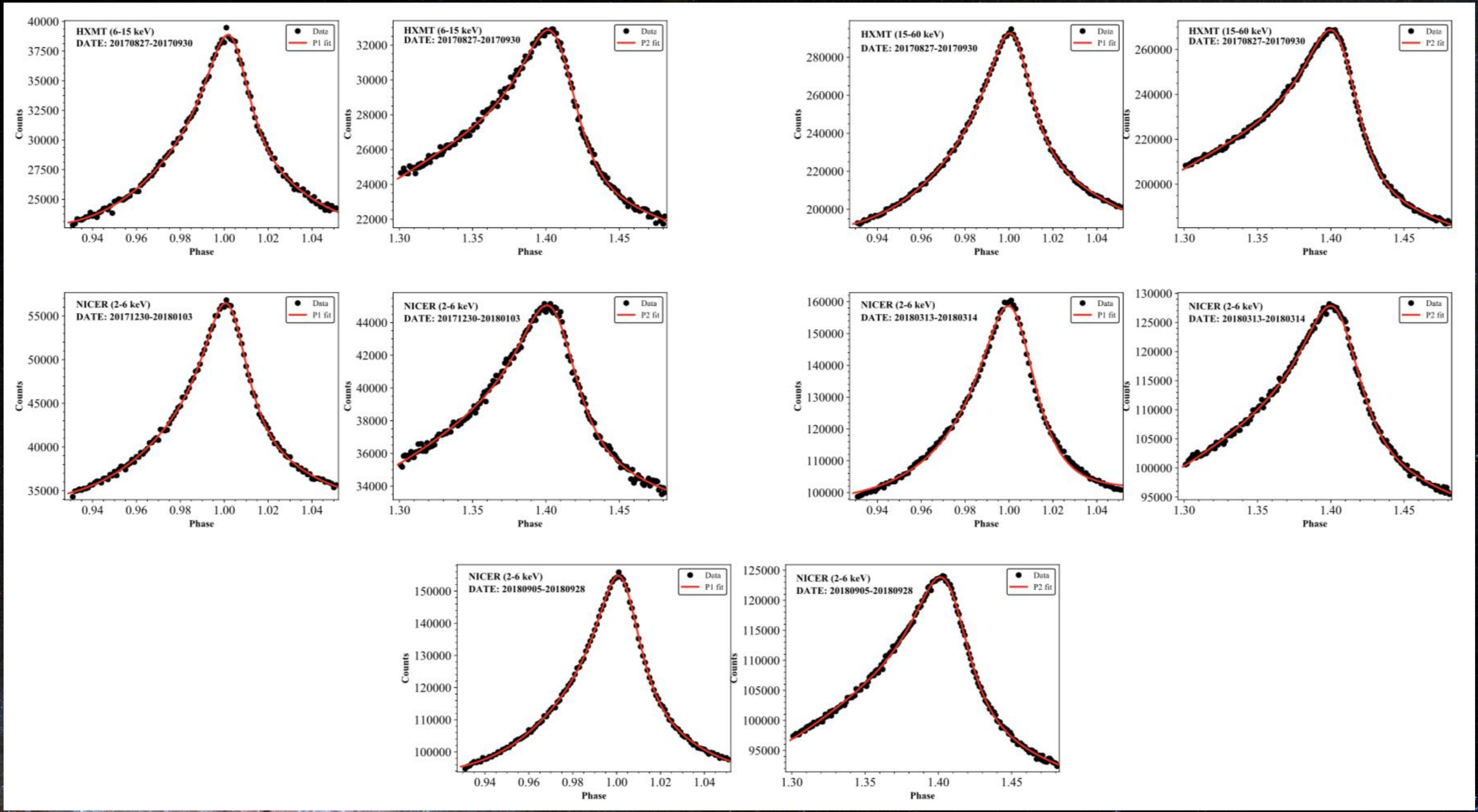

Empirical formula（Nelson et al. 1970） $$F(\phi-\phi_0) = H\frac{1+c_1(\phi-\phi_0)+c_2(\phi-\phi_0)^2}{1+c_3(\phi-\phi_0)+c_4(\phi-\phi_0)^2}e^{-c_5*(\phi-\phi_0)^2}+l,$$

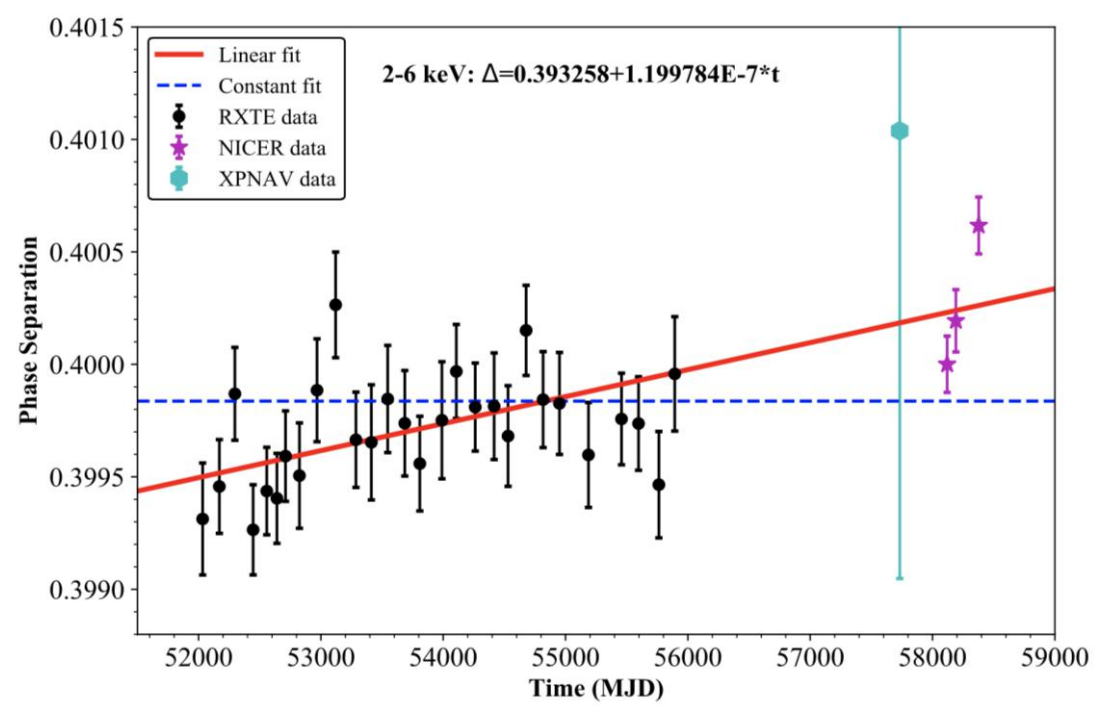

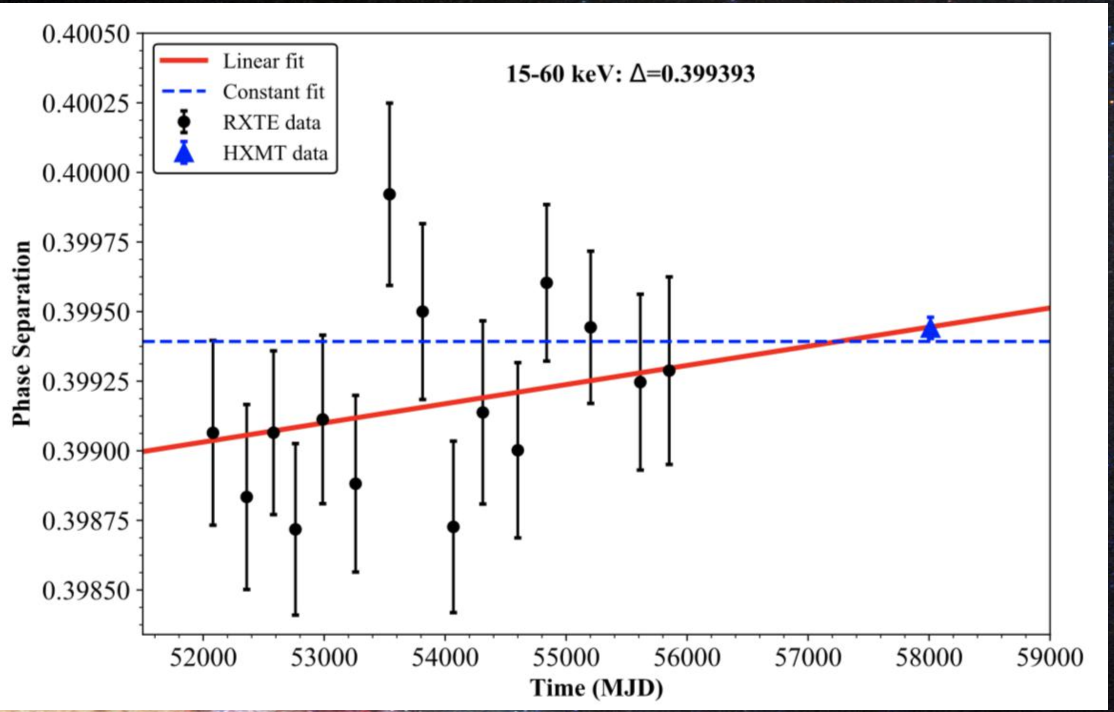

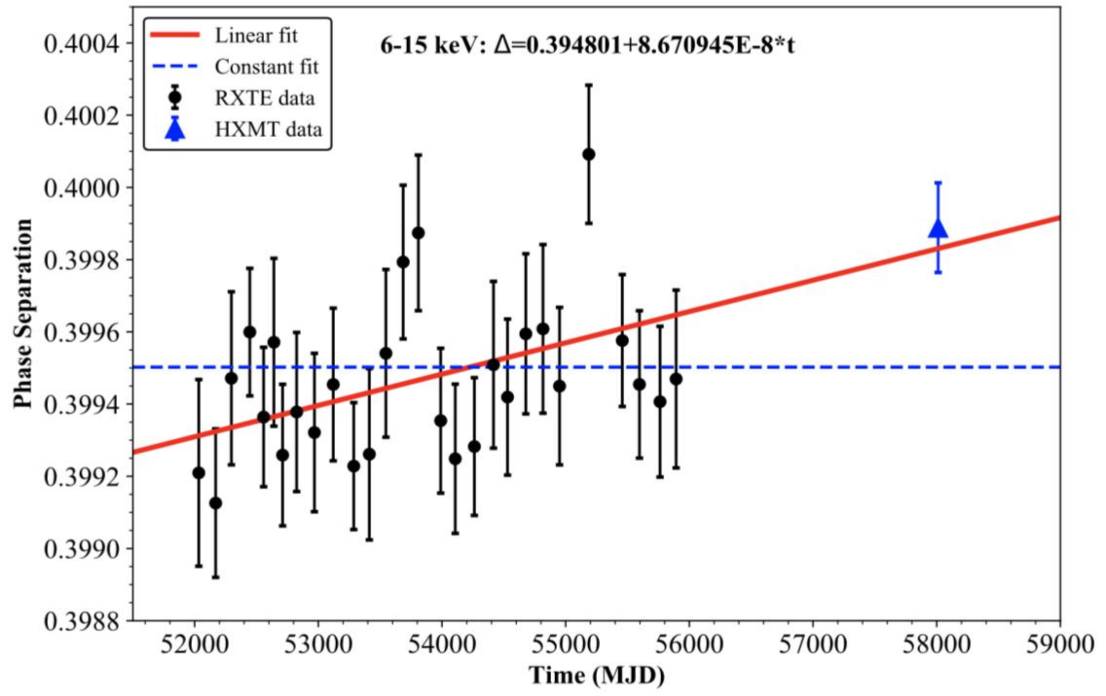

Evolution of phase separation (Δ) of two peaks for the Crab pulsar in the three x-ray bands

Preliminary results

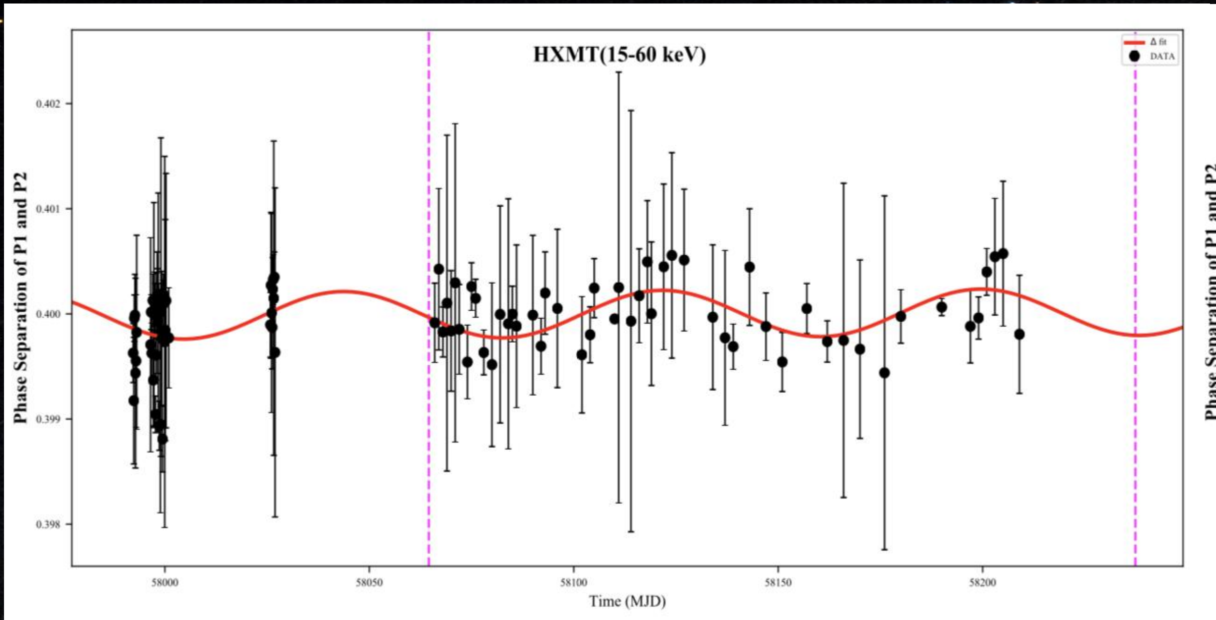

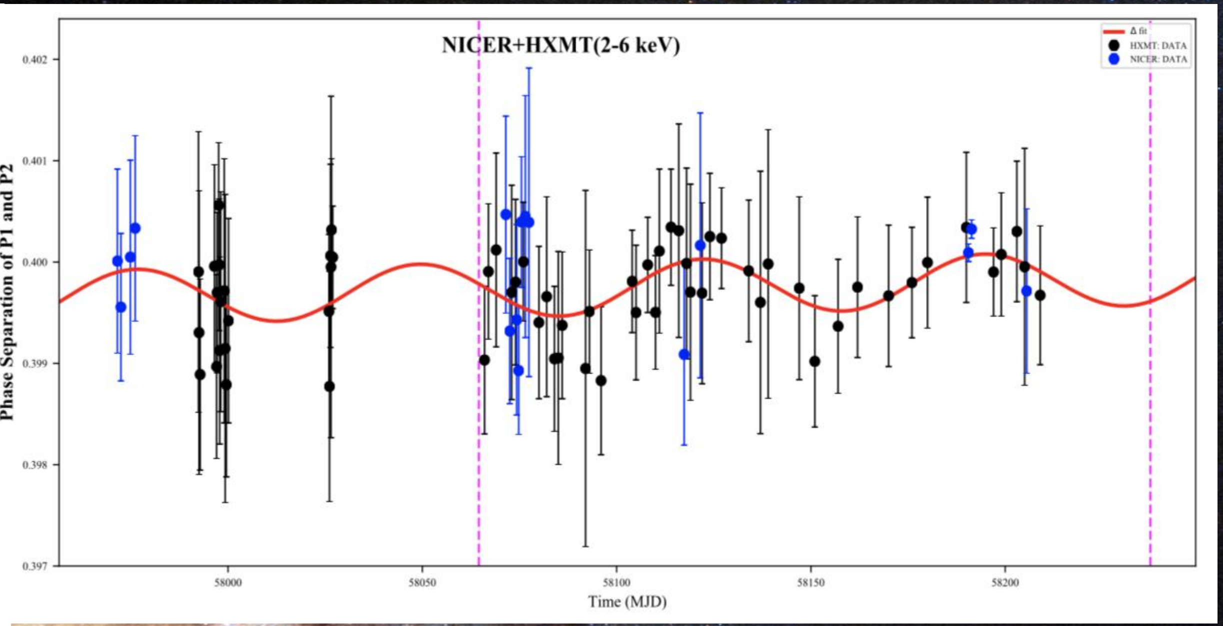

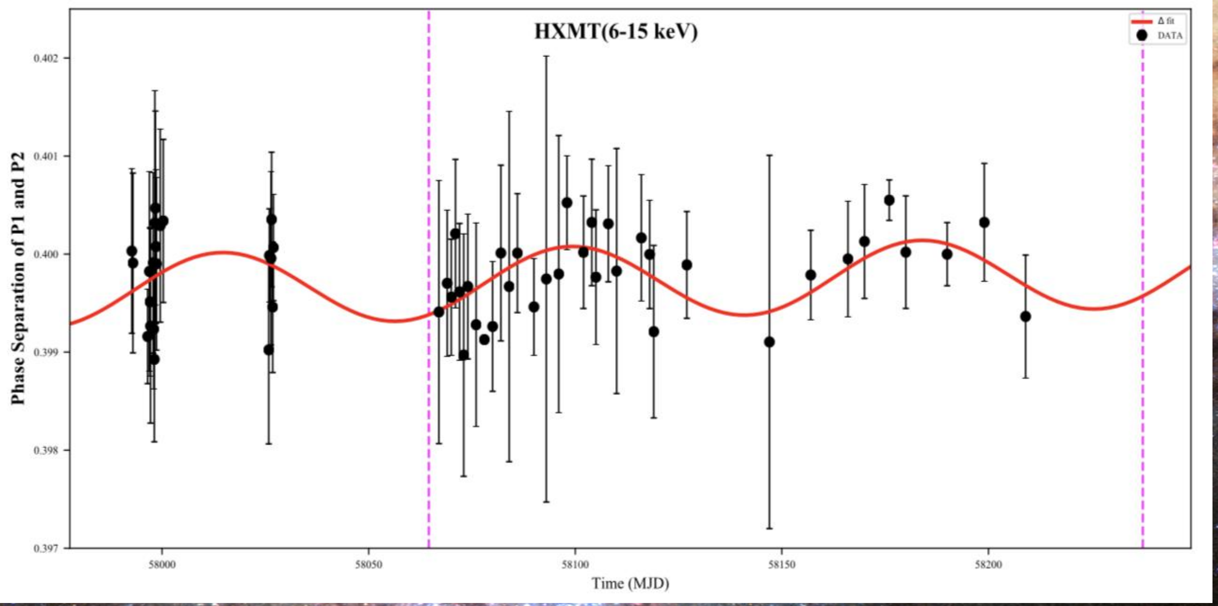

Evolution of phase separation Δ of two peaks for the Crab pulsar in HE, ME, LE bands.

Preliminary results

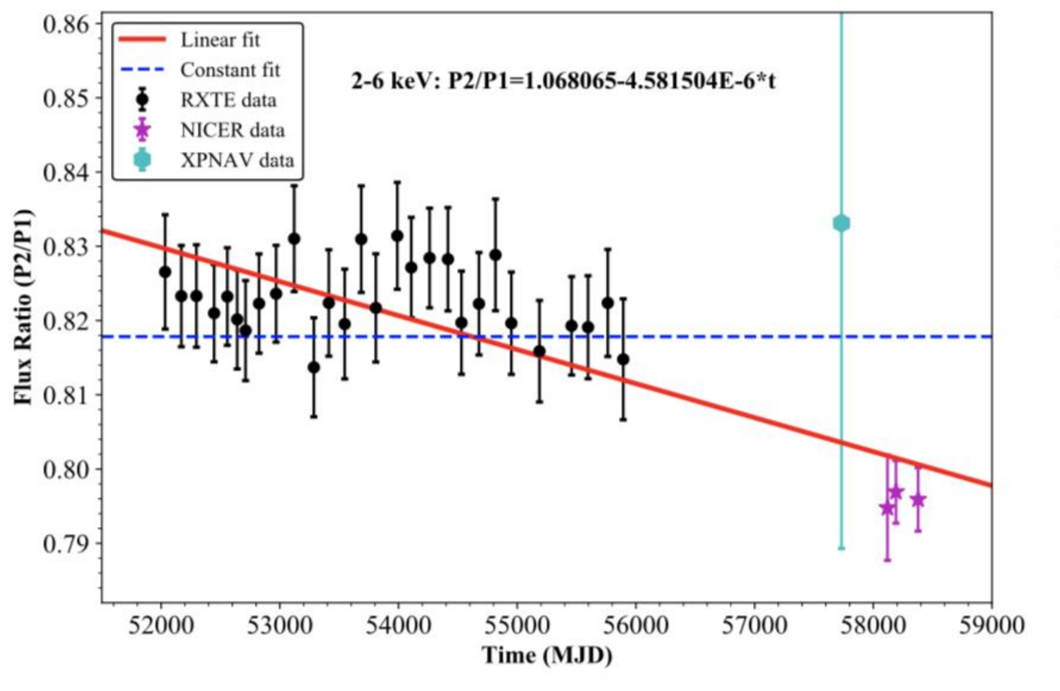

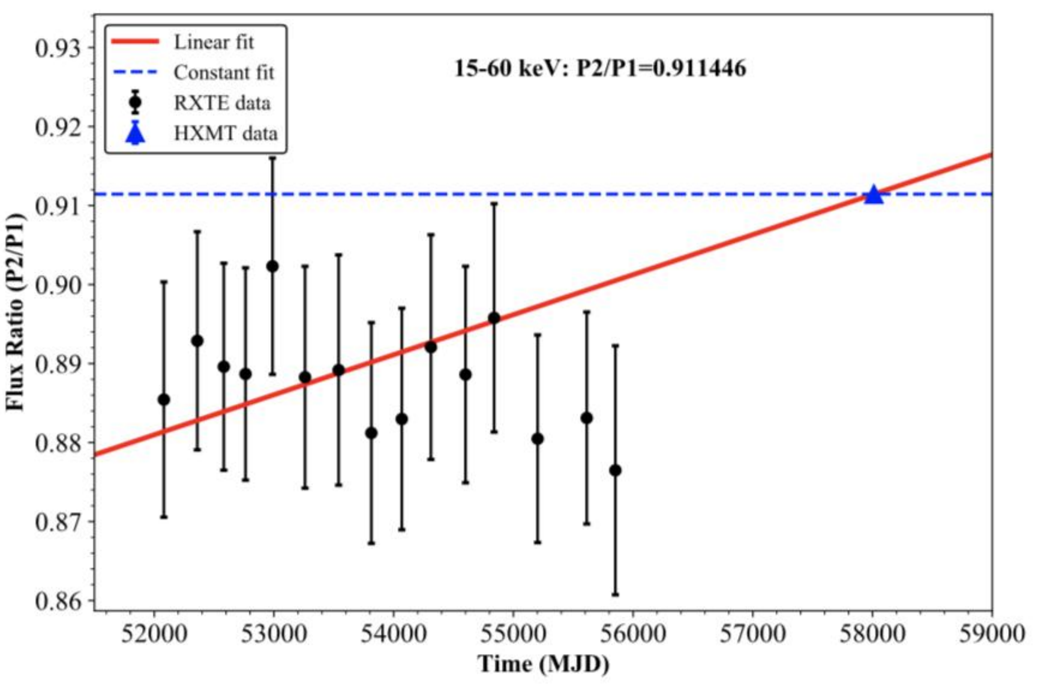

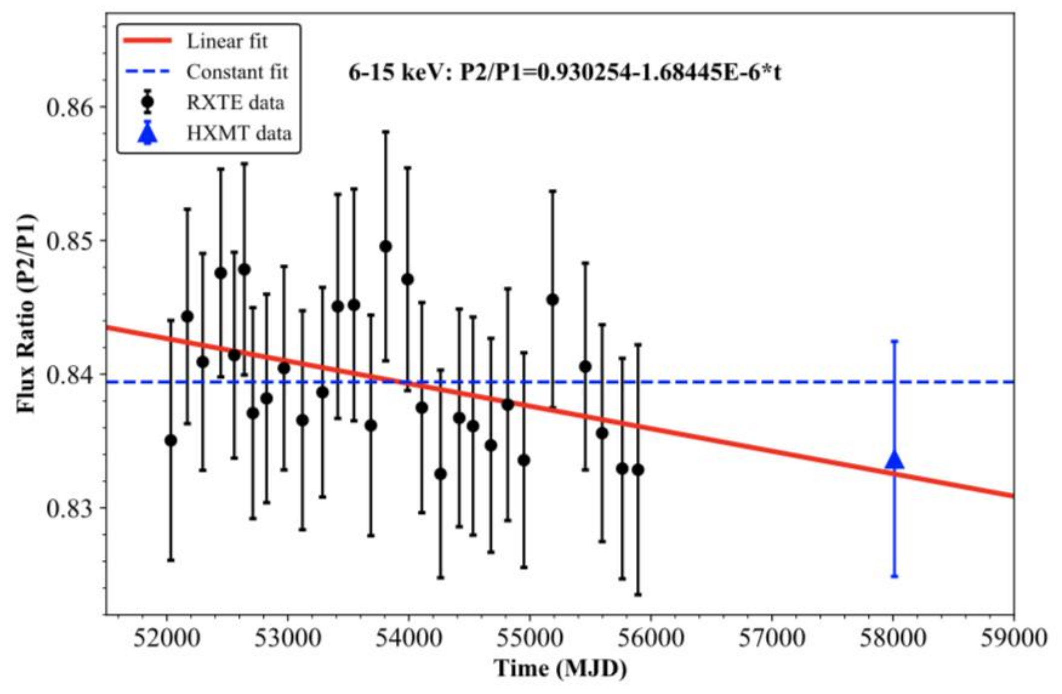

Evolution of the flux ratio (P2/P1) for the Crab pulsar in the three X-ray bands

Preliminary results

Possible interpretations for the secular variations of the pulse profile:

- Precession
- Change in Inclination angle α
- The location within the magnetosphere of the source of emission

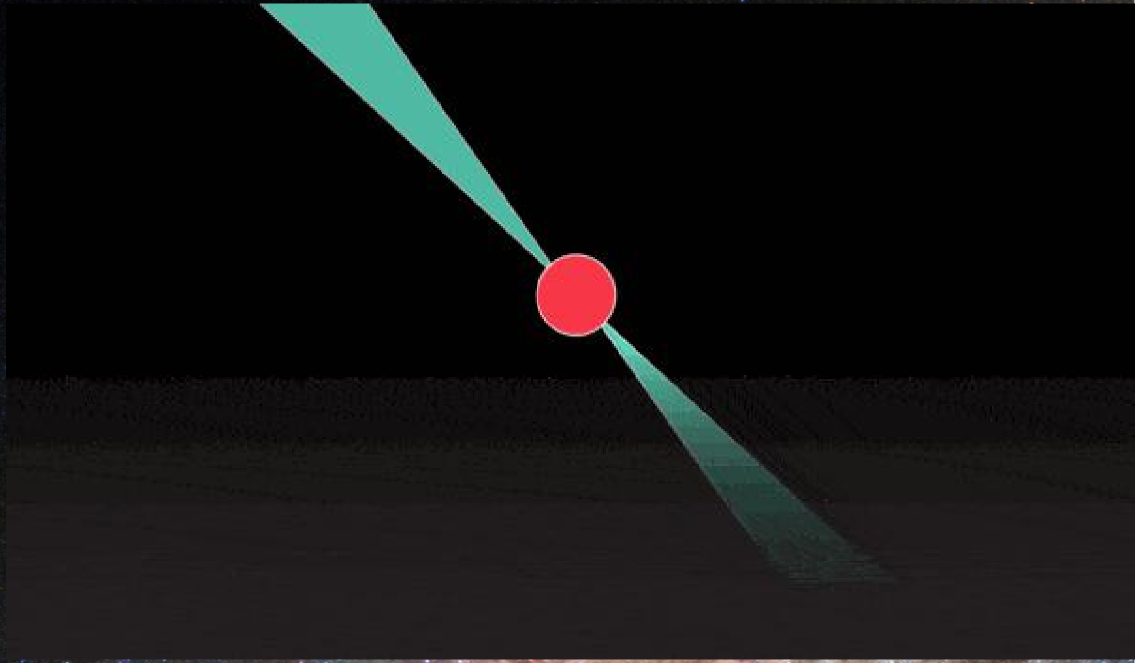

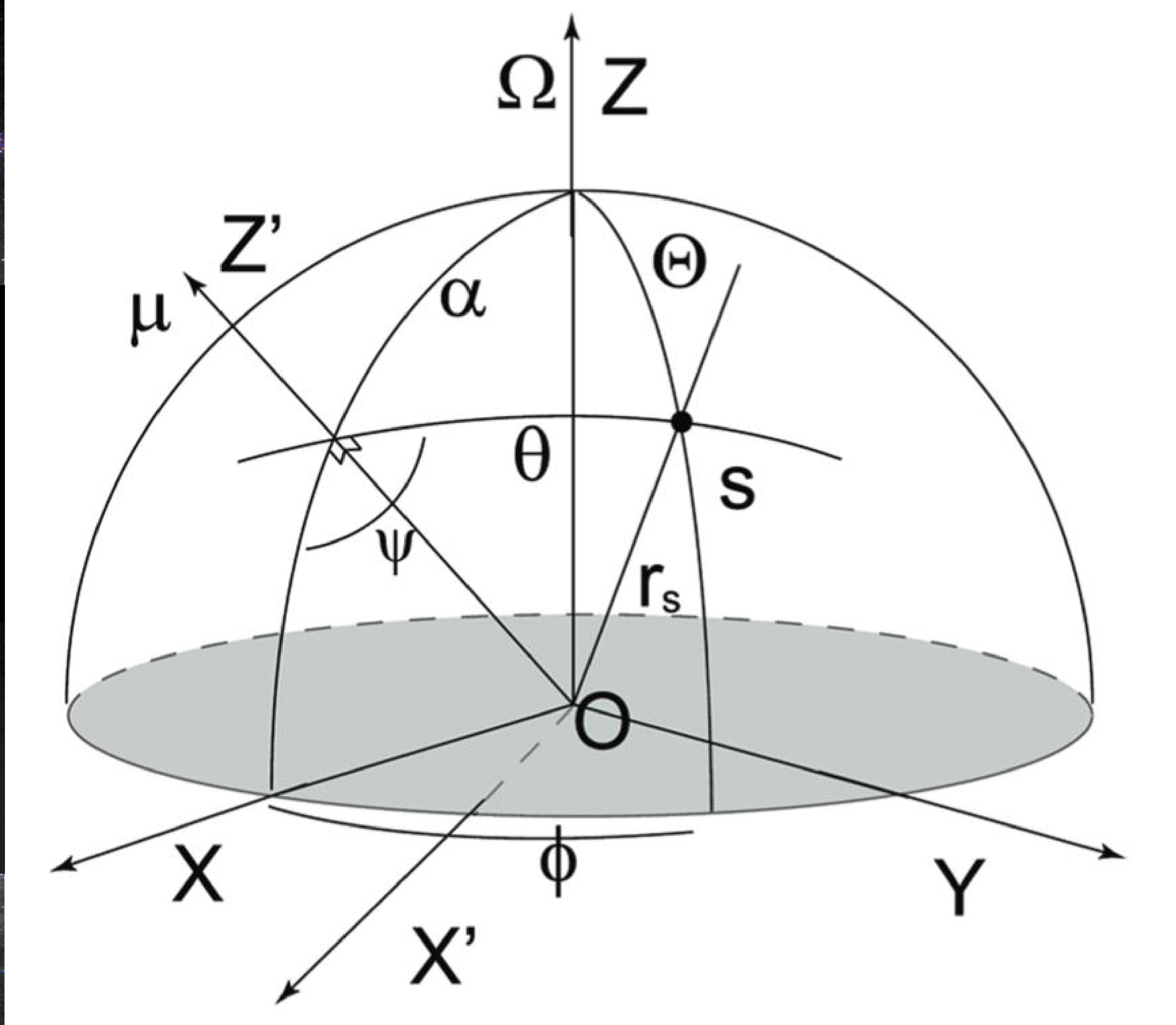

Lee et al. 2010

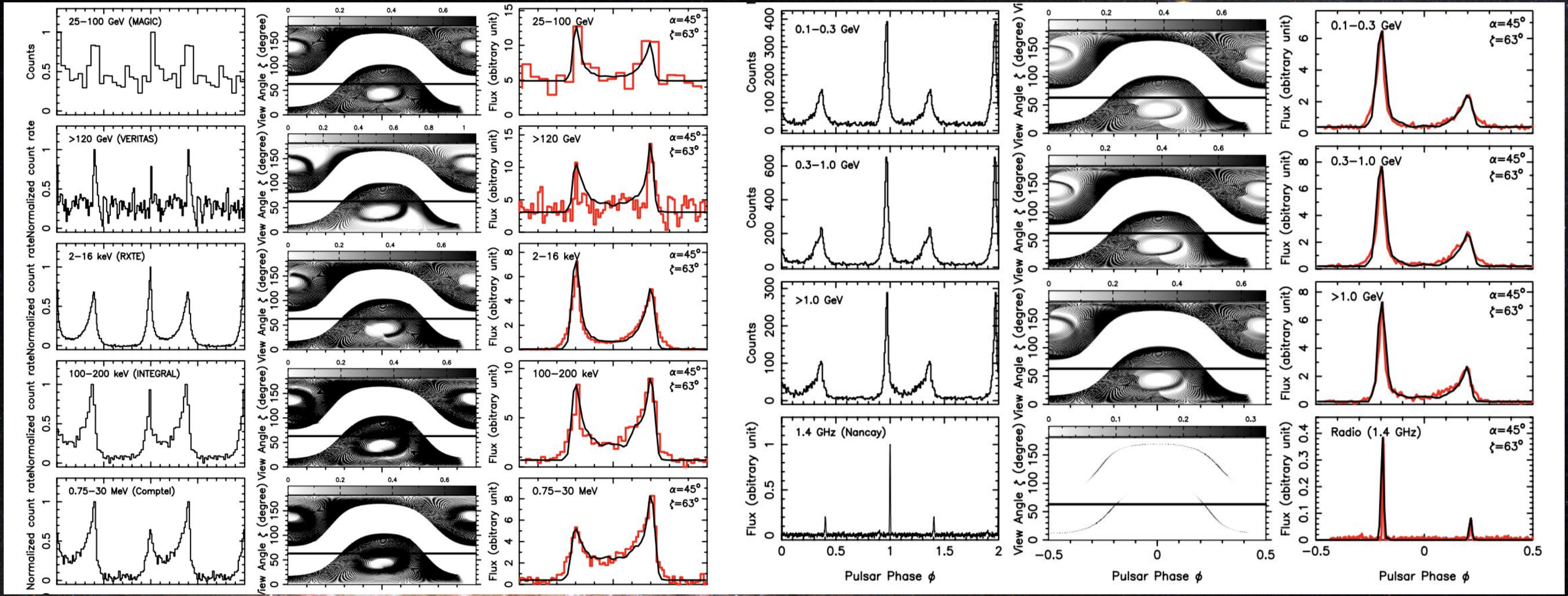

Multi-wavelength (radio, X-ray, and γ -ray) light curves for the Crab pulsar. (Du et al. 2012)

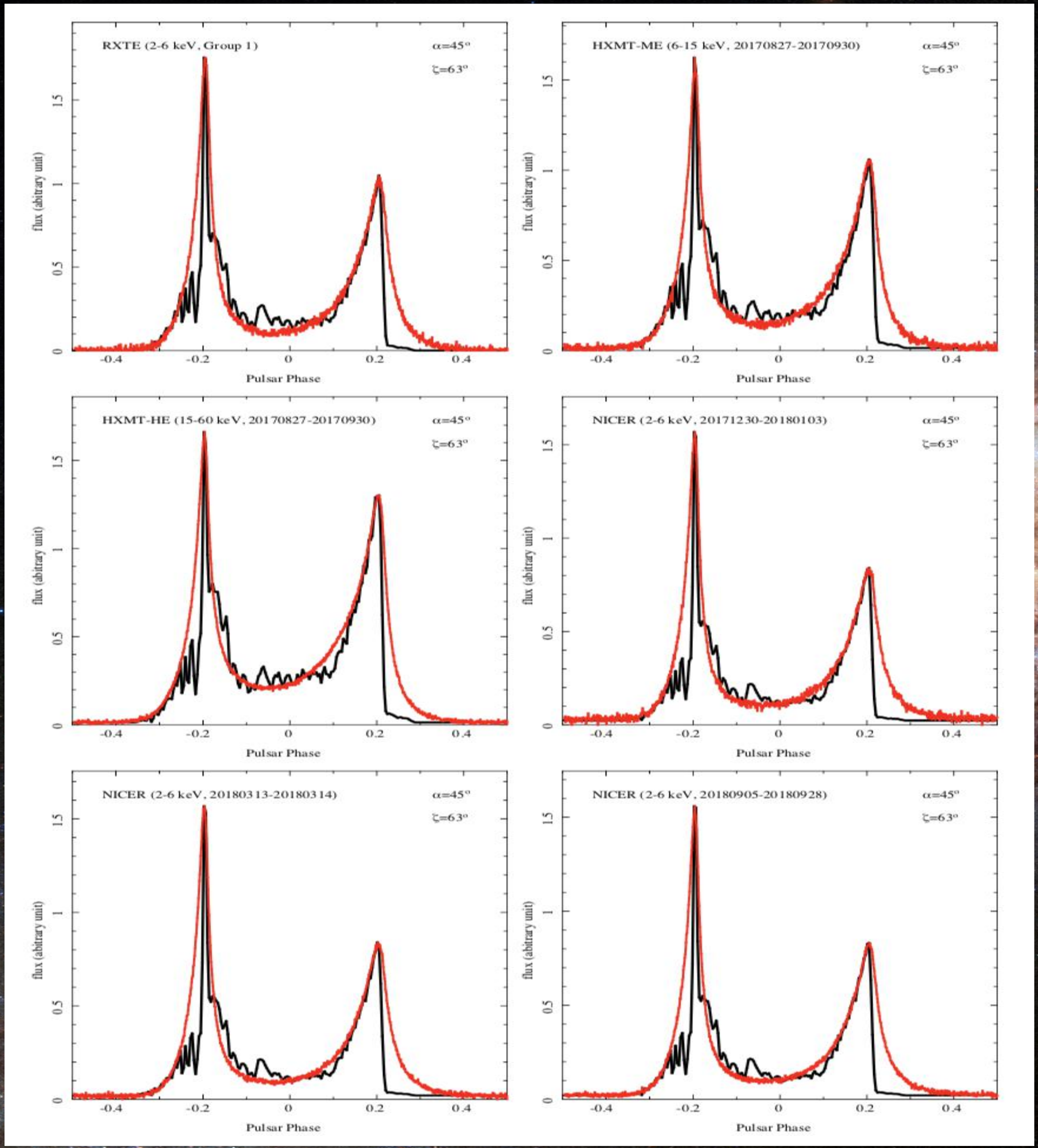

Modelling the pulse profile of the Crab pulsar using the AG model

Preliminary results

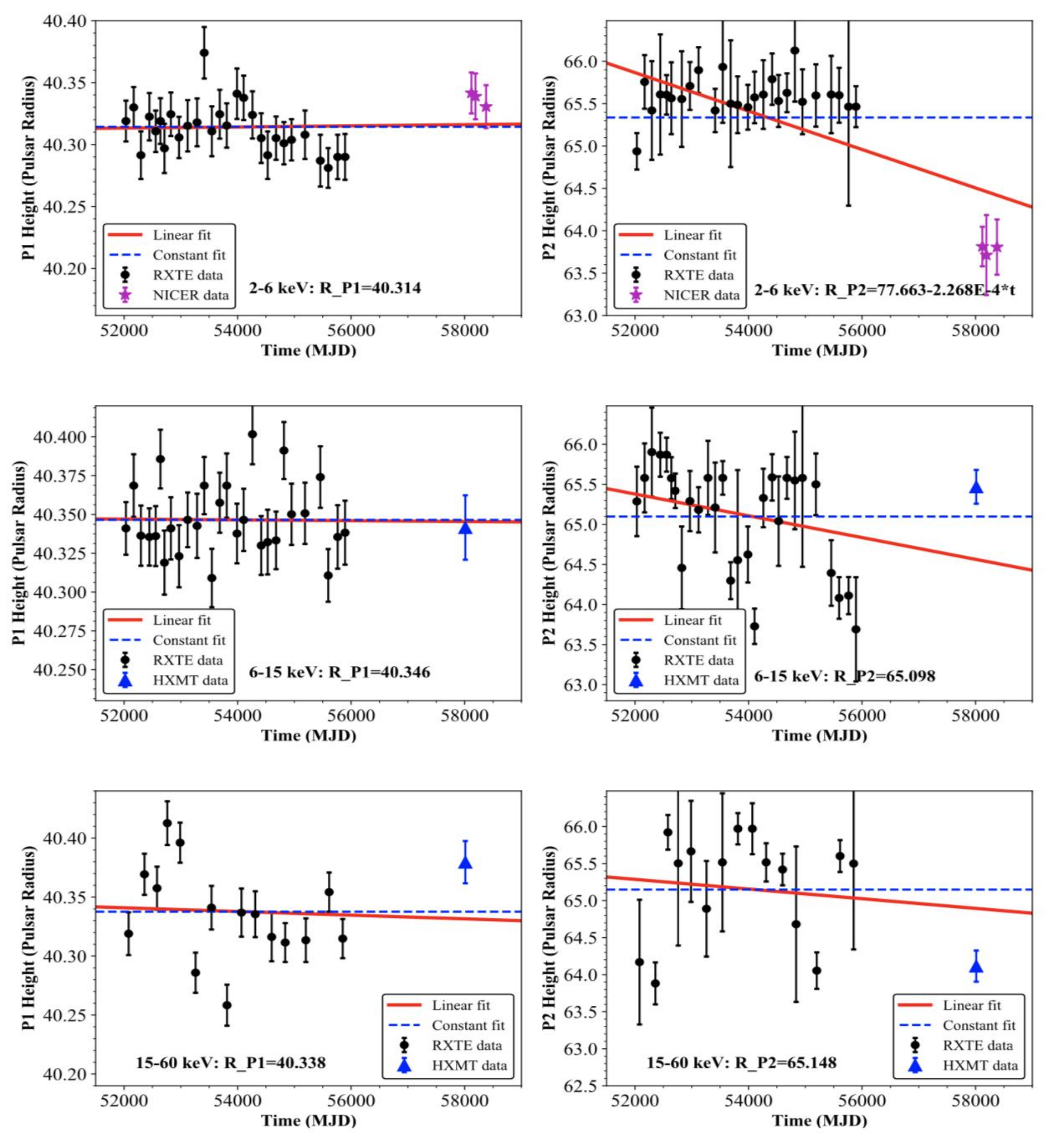

Evolution of maximum emission heights of P1 and P2 simulated with the AG model in the three X-ray bands

Preliminary results

IV. Summary

X-ray band	Linear model (LM)						Constant model (CM)			F-test		Change rate of Δ
	Parameter	Value	Error	χ^2_{LM}/dof	T_{LM}	$Pvalue_{LM}$	Value	Error	χ^2_{CM}/dof	Fvalue	Pvalue	(deg/century)
2−6 keV	*a* *b*	3.933E-1 1.200E-7	1.082E-3 1.972E-8	39.077/29	4.918	1.593E-5	3.998E-1	6.244E-5	88.939/30	18.485	3.748E-4	1.577 ±0.259
6−15 keV	*a* *b*	3.948E-1 8.671E-8	1.241E-3 2.288E-8	26.158/27	3.184	1.817E-3	3.995E-1	4.533E-5	40.078/28	7.449	2.247E-2	1.139 ±0.301
15−60 keV	*a* *b*	3.955E-1 6.880E-8	1.189E-3 2.076E-8	14.217/14	1.310	1.056E-1	3.994E-1	4.485E-5	25.364/15	2.599	2.619E-1	0.904 ±0.273

X-ray band	Linear model (LM)						Constant model (CM)			F-test		Change rate of P2/P1
	Parameter	Value	Error	χ^2_{LM}/dof	T_{LM}	$Pvalue_{LM}$	Value	Error	χ^2_{CM}/dof	Fvalue	Pvalue	(per century)
2−6 keV	*a* *b*	1.068 -4.582E-6	3.130E-2 5.726E-7	27.365/29	-6.579	1.646E-7	8.178E-1	2.031E-3	87.770/30	30.227	1.425E-5	-0.167 ± 0.0209
6−15 keV	*a* *b*	9.303E-1 -1.684E-6	3.488E-2 6.466E-7	8.722/27	-2.640	6.805E-3	8.394E-1	9.440E-4	10.915/28	6.520	3.375E-2	-0.0615 ± 0.0236
15−60 keV	*a* *b*	6.175E-1 5.067E-6	3.802E-2 6.553E-7	8.646/14	2.741	7.958E-2	9.114E-1	5.991E-7	45.568/15	5.951	6.229E-1	—

X-ray band	Linear model (LM)						Constant model (CM)			F-test		Good model
	Parameter	Value	Error	χ^2_{LM}/dof	T_{LM}	$Pvalue_{LM}$	Value	Error	χ^2_{CM}/dof	Fvalue	Pvalue	
2−6 keV	$a_{R_{P1}}$ $b_{R_{P1}}$	40.289 4.576E-7	1.100E-1 2.025E-6	34.295/29	2.212E-1	4.167E-1	40.314	3.514E-3	34.355/30	5.884E-3	1.212E-1	CM
	$a_{R_{P2}}$ $b_{R_{P2}}$	77.663 -2.268E-4	2.598 4.778E-5	54.576/27	-4.713	3.293E-5	65.337	1.148E-1	100.139/28	23.457	1.017E-4	LM
6−15 keV	$a_{R_{P1}}$ $b_{R_{P1}}$	40.360 -2.539E-7	1.743E-1 3.230E-6	39.603/27	-8.103E-2	4.680E-1	40.346	4.268E-3	39.612/28	8.103E-2	5.320E-1	CM
	$a_{R_{P2}}$ $b_{R_{P2}}$	72.443 -1.358E-4	4.429 8.188E-5	130.545/27	-1.597	6.095E-2	65.098	1.309E-1	143.853/28	4.005	1.118E-1	CM
15−60 keV	$a_{R_{P1}}$ $b_{R_{P1}}$	40.422 -1.563E-6	3.722E-1 6.875E-6	77.352/14	-2.274E-1	4.109E-1	40.338	1.001E-2	77.616/15	4.800E-2	3.400E-1	CM
	$a_{R_{P2}}$ $b_{R_{P2}}$	68.681 -6.527E-5	6.782 1.253E-4	96.711/14	-5.211E-1	3.033E-1	65.148	1.839E-1	106.303/15	2.521E-1	7.520E-1	CM


Thank you!